

## Large volume high-pressure cell for inelastic neutron scattering

W. Wang, D. A. Sokolov, A. D. Huxley, and K. V. Kamenev

Citation: *Rev. Sci. Instrum.* **82**, 073903 (2011); doi: 10.1063/1.3608112

View online: <http://dx.doi.org/10.1063/1.3608112>

View Table of Contents: <http://rsi.aip.org/resource/1/RSINAK/v82/i7>

Published by the [American Institute of Physics](#).

---

### Related Articles

A cryogenic high pressure cell for inelastic neutron scattering measurements of quantum fluids and solids  
*Rev. Sci. Instrum.* **84**, 015101 (2013)

TOF-SEMSANS—Time-of-flight spin-echo modulated small-angle neutron scattering  
*J. Appl. Phys.* **112**, 014503 (2012)

A high temperature high pressure cell for quasielastic neutron scattering  
*Rev. Sci. Instrum.* **82**, 083903 (2011)

Rheo—small-angle neutron scattering at the National Institute of Standards and Technology Center for Neutron Research  
*Rev. Sci. Instrum.* **82**, 083902 (2011)

A spin-echo resolved grazing incidence scattering setup for the neutron interrogation of buried nanostructures  
*Rev. Sci. Instrum.* **80**, 123903 (2009)

---

### Additional information on *Rev. Sci. Instrum.*

Journal Homepage: <http://rsi.aip.org>

Journal Information: [http://rsi.aip.org/about/about\\_the\\_journal](http://rsi.aip.org/about/about_the_journal)

Top downloads: [http://rsi.aip.org/features/most\\_downloaded](http://rsi.aip.org/features/most_downloaded)

Information for Authors: <http://rsi.aip.org/authors>

## ADVERTISEMENT

**JANIS** Does your research require low temperatures? Contact Janis today.  
Our engineers will assist you in choosing the best system for your application.



10 mK to 800 K      LHe/LN<sub>2</sub> Cryostats  
Cryocoolers      Magnet Systems  
Dilution Refrigerator Systems  
Micro-manipulated Probe Stations

[sales@janis.com](mailto:sales@janis.com)    [www.janis.com](http://www.janis.com)  
Click to view our product web page.

## Large volume high-pressure cell for inelastic neutron scattering

W. Wang,<sup>1</sup> D. A. Sokolov,<sup>2</sup> A. D. Huxley,<sup>2</sup> and K. V. Kamenev<sup>1,a)</sup>

<sup>1</sup>Centre for Science at Extreme Conditions and School of Engineering, University of Edinburgh, Edinburgh EH9 3JZ, United Kingdom

<sup>2</sup>SUPA, Centre for Science at Extreme Conditions and School of Physics and Astronomy, University of Edinburgh, Edinburgh EH9 3JZ, United Kingdom

(Received 19 May 2011; accepted 15 June 2011; published online 15 July 2011)

Inelastic neutron scattering measurements typically require two orders of magnitude longer data collection times and larger sample sizes than neutron diffraction studies. Inelastic neutron scattering measurements on pressurised samples are particularly challenging since standard high-pressure apparatus restricts sample volume, attenuates the incident and scattered beams, and contributes background scattering. Here, we present the design of a large volume two-layered piston-cylinder pressure cell with optimised transmission for inelastic neutron scattering experiments. The design and the materials selected for the construction of the cell enable its safe use to a pressure of 1.8 GPa with a sample volume in excess of 400 mm<sup>3</sup>. The design of the piston seal eliminates the need for a sample container, thus providing a larger sample volume and reduced absorption. The integrated electrical plug with a manganin pressure gauge offers an accurate measurement of pressure over the whole range of operational temperatures. The performance of the cell is demonstrated by an inelastic neutron scattering study of UGe<sub>2</sub>. © 2011 American Institute of Physics. [doi:10.1063/1.3608112]

### I. INTRODUCTION

Inelastic neutron scattering (INS) is an experimental technique commonly used in condensed matter research to study atomic and molecular motion as well as magnetic and crystal field excitations and lattice dynamics.<sup>1</sup> INS experiments are routinely performed at large-scale neutron facilities over a range of temperatures ( $T$ ) and magnetic fields ( $H$ ). Pressure ( $P$ ) is varied much less often because of the lack of the necessary equipment and the time it takes to conduct the measurements. However, pressure is an important thermodynamic parameter that can be used to tune magnetic, crystal field, and other parameters to gain insight into the microscopic physics of many phenomena.

In materials, in which interesting phenomena cease to exist at ambient pressure,  $P$  is not just a desirable but an essential tool for studies. For example, in UGe<sub>2</sub> superconductivity has been found to coexist with ferromagnetism below 1 K in a limited pressure range between 0.8 and 1.6 GPa.<sup>2,3</sup> The occurrence of superconductivity is correlated with a magnetic transition within the ferromagnetic state suggesting that critical fluctuations associated with this transition provide the microscopic pairing mechanism driving superconductivity.

These fluctuations are expected to be the strongest at the critical point of this transition, reached at pressure  $P_x = 1.2$  GPa and temperature  $T_x \approx 5$  K. INS at ambient pressure has already revealed that fluctuations of the uniform magnetisation associated with the Curie temperature are unusually strongly damped.<sup>4,5</sup> A pressure study would determine both the modification of these fluctuations and the spectrum of critical fluctuations at  $(P_x, T_x)$  to elucidate the mechanism responsible for the unusual form of superconductivity observed in the ferromagnetic state.

Here, we report on the pressure cell, we have built, suitable for the INS study of UGe<sub>2</sub> and capable of covering the whole  $P$ - $T$ -phase diagram of this material. The design challenges are outlined in Sec. II.

### II. DESIGN CHALLENGES

There are two major impediments in conducting neutron scattering experiments at high pressure. The first one is the limited size of the sample space inside the pressure cell. The second is the attenuation of the neutron beam passing through the walls of the cell combined with increased background scattering. These problems are relevant to both elastic and inelastic neutron scattering, but in combination with the longer data collection times necessary for INS, they create a substantial barrier in performing such measurements.<sup>6,7</sup> Next, we review the limitations of existing cell designs.

Gas pressure cells have the advantage of permitting a fine control of the pressure.<sup>8,9</sup> For modest pressures below 0.6 GPa and room temperature, large sample volumes are possible and aluminium alloys can be used for the cell construction to minimize neutron absorption. These cells are therefore the best choice for applications restricted to these parameters. Although helium does not solidify at room temperature until 11.5 GPa,<sup>10</sup> safe external handling of pressurised gases limits the pressures attainable with these cells to around 0.6 GPa. The pressure is also hard to set at low temperature since the solidification pressure for helium, although the highest for any fluid at low temperature, falls rapidly as temperature is decreased and is only around 30 bars (3 MPa) at 2 K. The pressure is therefore locked at high temperature and the high compressibility and thermal expansion of solid helium complicate maintaining the pressure to low temperature. For the present purpose, the pressure limit of 0.6 GPa and low temperature requirement rules out the use of gas pressure cells.

<sup>a)</sup>Electronic mail: K.Kamenev@ed.ac.uk.

Opposed anvil pressure cells such as those based on the Paris-Edinburgh press<sup>11</sup> have been used for INS experiments to pressures of 10 GPa.<sup>12</sup> However, the sample volume is limited to 10–25 mm<sup>3</sup> and scattering from the anvils and the gasket results in a large background.

A pressure cell design that has the operational parameters close to our requirements in terms of its attenuation and the pressure attainable is the *Clamp 04PCL150CB5* cell available at the Institut Laue-Langevin (ILL, France).<sup>13</sup> The cell is made of BeCu alloy and can accommodate a 5 mm diameter and 20 mm long sample. It is claimed that the cell can achieve 1.5 GPa at room temperature,<sup>13</sup> and low-temperature studies performed in this cell at pressures of up to 1.2 GPa have been reported.<sup>14,15</sup> The yield strength of the fully hardened BeCu alloy is approximately 1.4 GPa (Ref. 16) indicating that at this pressure the cell is operating at its limit. The use of CrNiAl alloy in the construction of the clamped pressure cell was mentioned in a neutron diffraction study of MnSi to 1.3 GPa by B. Fåk *et al.*<sup>17</sup>

In order to cover the whole  $P$ - $T$ -phase diagram of UGe<sub>2</sub> and to reach  $P_x$  and  $T_x$ , we need to access pressures of 1.5 GPa at low temperatures. Taking into account the loss of pressure in the liquid pressure medium with cooling this translates to approximately 1.8 GPa at room temperature. Also, because of the narrow pressure interval spanned by the  $P_x, T_x$  phase transition line it is important to have an accurate measurement of pressure when the load is applied and the cell is clamped. In previous pressure cells used for neutron scattering,  $P$  was measured either by using a reference material with known equation of state, e.g., NaCl,<sup>18</sup> or using a calibrated transition temperature, e.g., Pb, Sn, or In.<sup>19</sup> In the first case the added reference reduces the volume of the sample, risks “contaminating” the neutron scattering from the sample, and in studies of single-crystals using a three-axis spectrometer requires additional alignment of the reference. The use of a calibrated transition in Pb, Sn, or In has the advantage of allowing pressure verification without the neutron beam, but the pressure can be measured only at the transition temperature of the reference material. Additionally, the pressure cell needs to be made of non-magnetic materials in order not to disturb the magnetic field at the reference position.

Another design factor is that the cell should permit single-crystal samples to be mounted and held in a well maintained orientation. In Sec. III, we present the design of the large volume piston-cylinder pressure cell for INS experiments which addresses the various issues outlined above.

### III. DESIGN AND MATERIAL SELECTION

The cross-sectional view of the pressure cell with its key dimensions is presented in Fig. 1. The main components of the cell are a cylindrical body, a plug with electrical feed-through, a piston, a locking nut, and a spacer which prevents the piston from rotating when the locking nut is tightened. All the parts are made of non-magnetic materials. The pusher, piston, and spacer are made of non-magnetic tungsten carbide Roctec 500.<sup>20</sup> The locking nut, the plug, and the outer

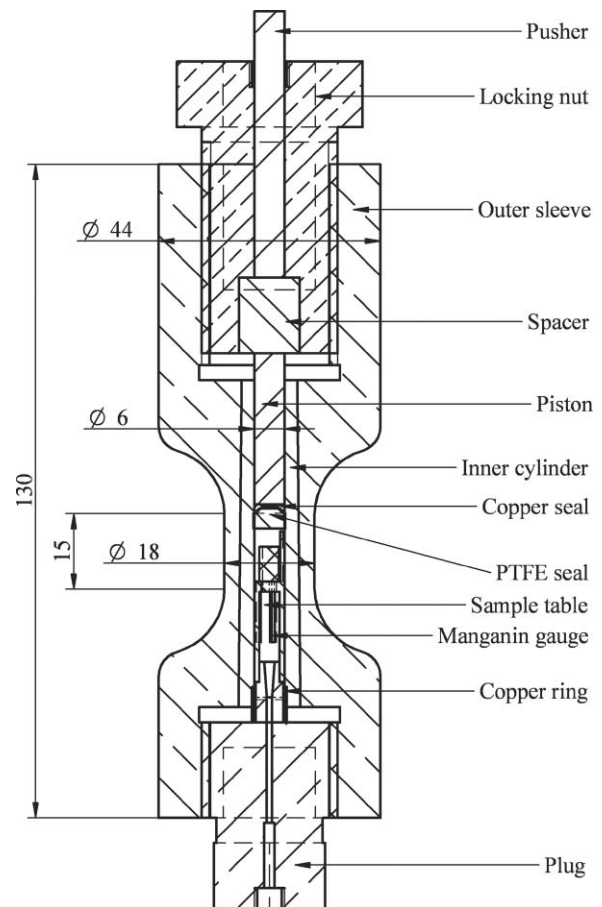


FIG. 1. Cross-sectional view of the pressure cell assembly (dimensions are in mm). The dimensions are to scale but note that the overall length of the cell depends on the position of the locking nut which changes with pressure.

sleeve are made of fully hardened BERYLCO-25 alloy (yield strength = 1.4 GPa) (Ref. 16) and the inner cylinder is made of CrNiAl alloy (yield strength = 2.1 GPa).<sup>21</sup>

The body of the pressure cell is 44 mm diameter and 130 mm long (Fig. 1), making it suitable for use with most cryostats, closed cycle refrigerators (CCRs), and cryomagnets. The sample space is optimised for 6 mm diameter and 15 mm long samples, thus accommodating a sample volume of  $\sim 425$  mm<sup>3</sup>. It is large enough to accommodate large single-crystals of UGe<sub>2</sub>. Pressure is generated in a hydraulic press by a removable tungsten carbide pusher and then locked by means of the locking nut.

#### A. Layered body and neck optimisation

The body of the cell consists of two parts—the inner cylinder and the outer sleeve. Both the bore of the outer sleeve and the outer surface of the inner cylinder are machined with 1:50 taper and the inner cylinder is pressed into the outer cylinder with a 0.05 mm interference fit. The idea of a supported cylinder has been used in high-pressure cell design extensively in the past, and it is well-established that a two-layered pressure cell can generate higher pressure than a single-cylinder device.<sup>22</sup> This enabled us to have a neck on the outer cylinder to minimize the neutron attenuation

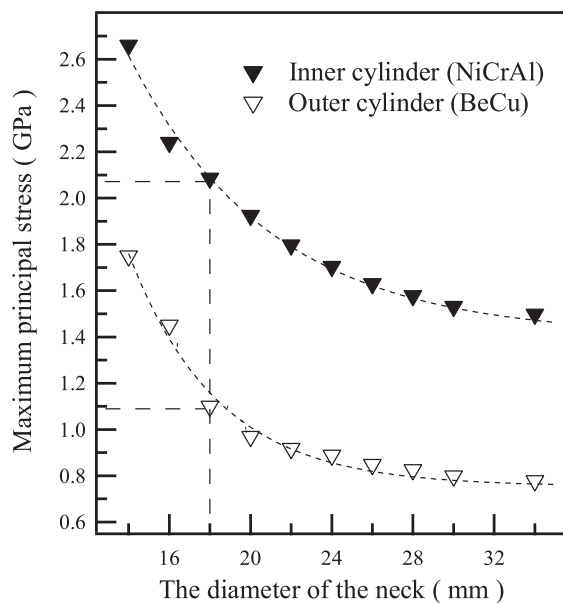


FIG. 2. Calculated maximum stress in the inner CrNiAl cylinder (filled triangles) and in the outer BeCu sleeve (open triangles) for pressure of 2.0 GPa applied to the sample. Dashed lines are the guide to eye.

without compromising the strength of the body. In order to minimize the amount of cell material in the neutron beam we have optimised the dimensions of the body using the ANSYS<sup>®</sup> finite element analysis (FEA) software.<sup>23</sup> A 3D model created with SOLID EDGE computer aided design package<sup>24</sup> was imported into ANSYS<sup>®</sup> and the appropriate boundary conditions were applied including the force modelling the interference fit between the two cylinders. To obtain accurate results, additional mesh refinement at the neck of the cell was included in the model.

For the fixed diameter of the inner bore ( $\phi 6$  mm) we have systematically analysed the stress distribution in the inner cylinder and in the outer sleeve by varying the diameter of the interface between the outer sleeve and the inner cylinder, and then varying the outer diameter of the outer cylinder at the neck of the cell. We found that the optimum diameter at the interface of the two cylinders is 11 mm. The results of the FEA analysis of the maximum stress as a function of the neck diameter for fixed bore of the cell ( $\phi 6$  mm) and fixed interface diameter ( $\phi 11$  mm) are summarised in Fig. 2. This shows that for the neck diameter of 18 mm, the maximum stress in the CrNiAl cylinder is 2.1 GPa and in the BeCu cylinder it is 1.1 GPa. We chose this diameter for the safe operation of the cell because the stress of 2.1 GPa matches the yield strength of CrNiAl, while the stress of 1.1 GPa is some 20% lower than the yield strength of BeCu alloy of which the outer sleeve is made. One of the functions of the outer sleeve is to protect the user, and choosing its design stress to be lower than its yield strength adds to the safety margin in the event of failure of the inner sleeve.

Figure 3 presents a section view of the body of the cell and shows the stress distribution for the  $\phi 18$  mm neck at 2.0 GPa. The simulation shows that the cell can reach the pressure of 2.0 GPa in the sample volume before the stress in the inner cylinder becomes larger than the yield strength of

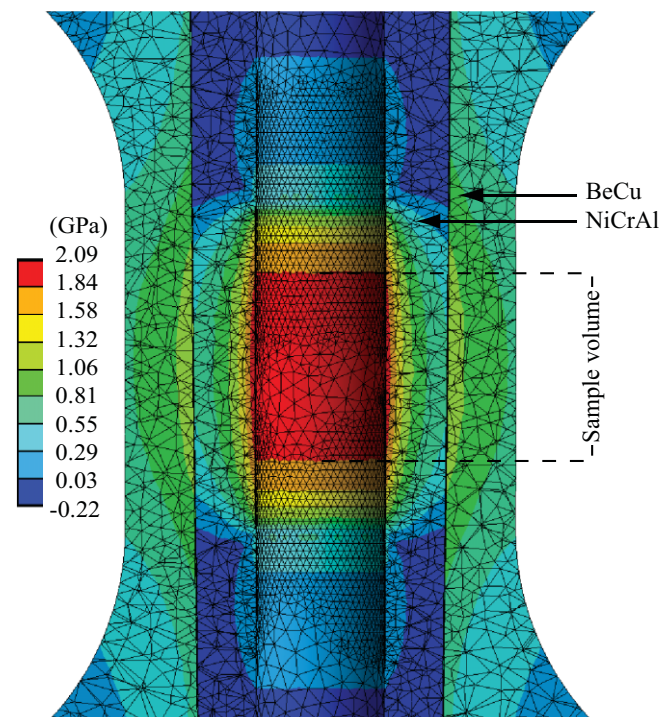


FIG. 3. (Color online) Section view of the 3D FEA model of the pressure cell body with maximum principal stress distribution as calculated for the sample pressure of 2 GPa.

CrNiAl. However, a safety margin of 10% should be applied and for safe use of the cell the working pressure should not exceed 1.8 GPa.

## B. Piston seal design

The piston was made of the binderless tungsten carbide Roctec 500 which performs well in compression and can withstand pressures over 2 GPa.<sup>20</sup> Difficulties with machining this ceramic material made it impossible to implement the conventional mushroom type seal conventionally used in piston-cylinder pressure cells. Another drawback of the mushroom seal is the use of soft metal seals made of indium, lead, or tin, which coat the bore of the cell, potentially increasing background neutron scattering. These metals are superconducting at low temperature and the onset of superconductivity might change the associated background signal over the range of temperatures of interest for measurement.

The above problem has been previously avoided by using a polytetrafluoroethylene (PTFE) capsule enclosing the sample and pressure transmitting medium.<sup>25,26</sup> However, the PTFE capsule takes up valuable sample space and scattering from it can be significant at the low-wave vectors associated with magnetic excitations.<sup>27</sup>

We approached the problem by implementing the seal shown in Fig. 4. The seal assembly consists of an oversized PTFE puck with a slight taper at one end for ease of insertion into the bore and an annealed copper anti-extrusion ring with a trapezoid cut-out profile. The operation of the seal is based on the unsupported area principle assured by the initial gap between the top tip of the PTFE puck and the inner edge of

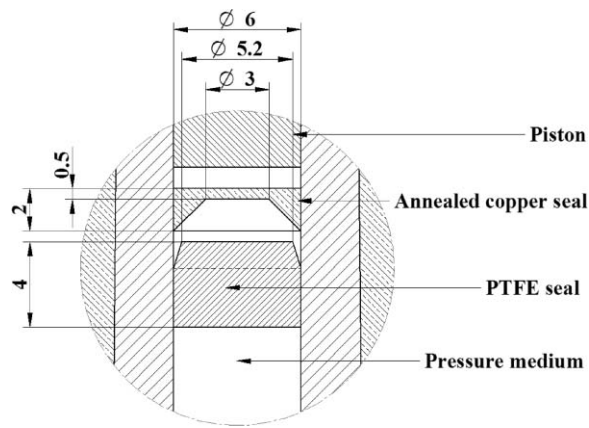


FIG. 4. Piston and seal assembly (dimensions are in mm). The piston, copper, and PTFE seals are shown in the initial position and are separated by small gaps for clarity.

the copper seal. The puck provides the seal at low pressures and generates enough force on the outer edge of the copper ring to seal at higher pressures. This design makes full use of the bore of the cell to accommodate the sample.

### C. Single-piece plug with manganin sensor

Often the load applied to the piston is not fully converted into the pressure inside the cell because of friction between the piston and the bore of the cell. In neutron scattering experiments, a reference material with a known equation of state is often used to determine the pressure *in situ*. However, the scattering from the reference can be confused with that of the sample. In order to measure the pressure inside the cell at any temperature with precision and avoid the interference from the pressure reference, we used a single-piece electrical plug (Fig. 1). The plug has copper feed-through wires which are used for measuring resistivity of the pressure sensor and also the resistivity of the sample in order to correlate the latter with changes in scattering. The copper wires are sealed inside the plug with Stycast 2850 FT epoxy manufactured by Emerson & Cumming Ltd. A single annealed copper ring on the neck of the plug provides an adequate seal for the pressure transmitting medium. An M6 threaded hole is made at the back of the plug for attaching the pressure cell to the cryogenics.

The pressure sensor is made of an enamelled manganin wire shaped into a coil with resistance of  $\sim 100 \Omega$ . Prior to use, the manganin coil was repeatedly cycled between the temperatures of 300 K and 2 K and subjected to the maximum pressure inside the pressure cell several times to relieve any thermal and stress hysteresis. Its electrical resistivity has been calibrated as a function of pressure for a wide range of temperatures.<sup>28</sup> The pressure applied to the sample can be determined with an accuracy better than  $\pm 0.01$  GPa by measuring the electrical resistivity of the manganin sensor by the four-probe technique. This accuracy is sufficient for mapping out the phase diagram of  $(P_x, T_x)$ .

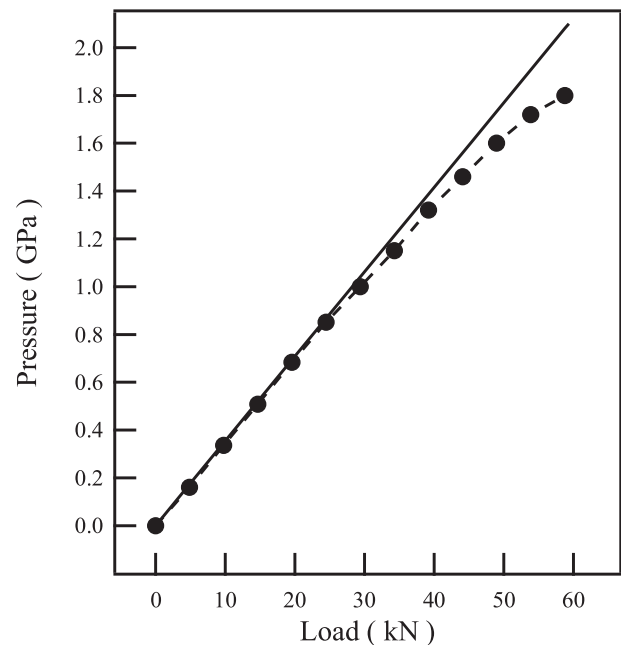


FIG. 5. Pressure-load performance of the cell. Filled circles are experimental data (the dashed line is the guide to the eye). The pressure and the load are measured using a manganin gauge (see text) and the load gauge of the press, respectively. The accuracy of determining the pressure is within  $\pm 0.01$  GPa and that of the load is  $\pm 0.15$  kN. The solid line is the ideal loading curve calculated from the applied force over the area of the piston.

### IV. ASSEMBLY AND TESTING

The assembly of the pressure cell starts with engaging the piston into the bore of the cell and backing it by the spacer and the locking nut. The copper seal and the PTFE puck are inserted through the opposite end of the cell and pushed through until they come into contact with the piston. The bore of the cell is then filled with the pressure medium and the plug with the sample is tightened to engage the copper seal on its neck. The pressure cell is placed into a safety shield and positioned between the piston and the anvil of a hydraulic press. Pressure is applied and monitored using the manganin sensor. Once the required pressure is reached, the locking nut is tightened and the load in the press is released.

The load dependence of pressure inside the cell at room temperature is shown in Fig. 5. Up to the pressure of  $\sim 1$  GPa the piston seal is virtually frictionless. At higher loads small frictional effects become noticeable. At the maximum pressure of 1.8 GPa the difference between the ideal loading curve (solid line in Fig. 5) and the actual pressure is  $\sim 0.2$  GPa, which is comparable to the best pressure-load performance achieved with a PTFE capsule.<sup>29</sup> We have found that the frictional effects can be further reduced by shortening the PTFE puck in the seal assembly but then the seal become less reliable and prone to occasional leaking.

We have also conducted a number of tests in which the pressure cell was cooled down to establish the drop in pressure due to the difference in the thermal expansion coefficients of the pressure cell and the pressure medium. The drop in the pressure has been estimated by applying a temperature correction to the pressure coefficient of the resistance of manganin.<sup>28</sup> It has been found that for the 1:1

mixture of FC72 and FC84 Fluorinerts<sup>TM</sup>, the pressure drop was  $\sim 0.3$  GPa between ambient temperature and 2 K.

## V. NEUTRON SCATTERING EXPERIMENT ON UGe<sub>2</sub>

Neutron scattering measurements were carried out on a single-crystal of UGe<sub>2</sub> (RRR = 70, mosaic = 1.2°) with the PANDA cold three-axis spectrometer at the Forschungs-Neutronenquelle Heinz Maier-Leibnitz, Germany. A mixture of FC72 and FC84 Fluorinerts<sup>TM</sup> providing quasi-hydrostatic conditions over the whole range of pressures and temperatures was used as the pressure transmitting medium. Measurements were performed using an open collimation configuration for the spectrometer to maximise flux. Fixed scattered energies  $k_f = 1.141 \text{ \AA}^{-1}$  and  $k_f = 2.282 \text{ \AA}^{-1}$  and cooled Be filter in the incident beam were used. The pressure cell was mounted on the cold plate of a standard CCR capable of reaching  $T = 3$  K. Temperature was measured by a Cernox<sup>TM</sup> thermometer. The incident beam was shielded from the body of the pressure cell away from the sample region by attaching Cd foil to the outside of the cell and appropriately adjusting the instrument apertures defining the incident beam.

To determine the neutron transmission of the pressure cell we measured a rocking curve of same single crystal of UGe<sub>2</sub> outside the pressure cell and under pressure of 1.4 GPa at room temperature at  $k_f = 2.282 \text{ \AA}^{-1}$  (Fig. 6). We note that the full width at half maximum (FWHM) of the rocking curve increases from 1.2° to 1.5° under pressure. Once the pressure is released the FWHM returns to 1.2°. The ratio of the integrated intensities at  $Q = 2\pi(0, 0, 1)/c$  is  $\sim 0.28$  indicating

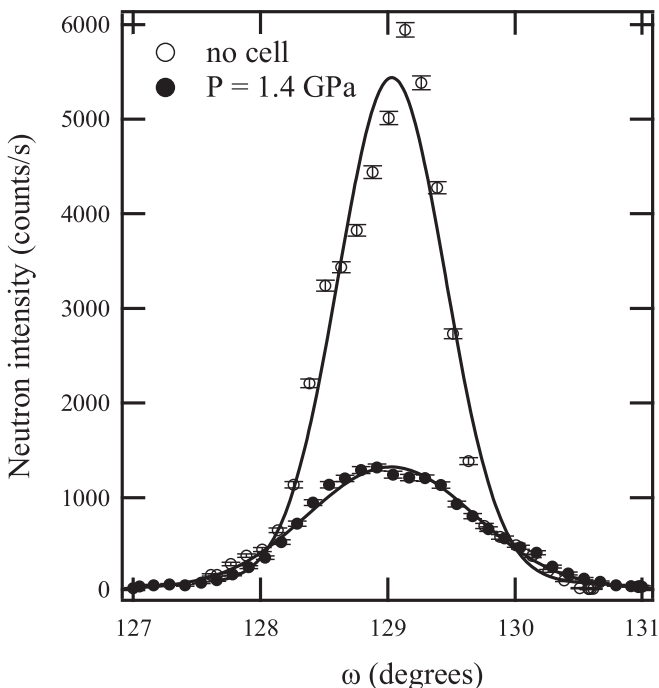


FIG. 6. Rocking curve of UGe<sub>2</sub> at  $Q = 2\pi(0, 0, 1)/c$  ( $k_f = 2.282 \text{ \AA}^{-1}$ ), collected at  $T = 297$  K at ambient pressure without the cell (open circles) and at  $P = 1.4$  GPa inside the cell (filled circles). Solid lines are the Gaussian fit of the data. Transmission of the cell is  $\sim 0.28$ .

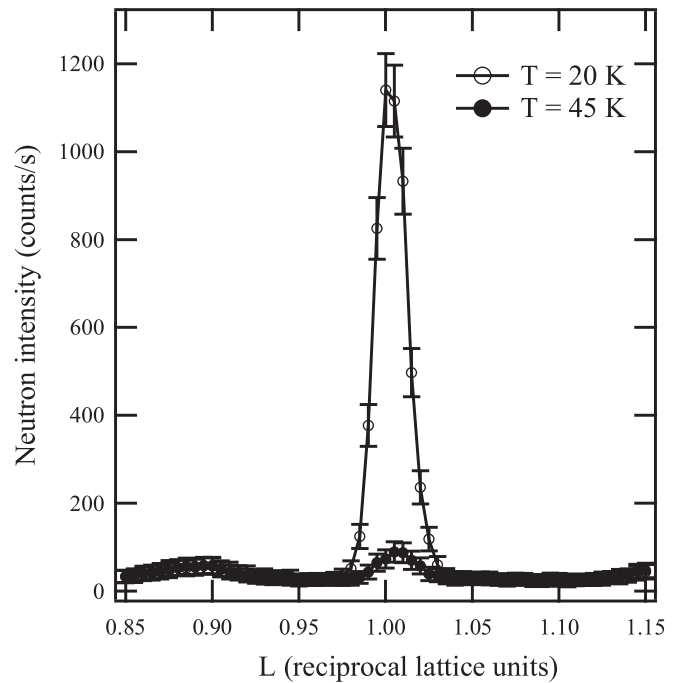


FIG. 7. Elastic longitudinal scan at  $k_f = 1.141 \text{ \AA}^{-1}$  through  $Q = 2\pi(0, 0, L)/c$  in UGe<sub>2</sub> collected at temperatures above and below the Curie temperature ( $T_C = 37$  K at  $P = 1.1$  GPa). The solid lines are the guide to the eye. Broad incommensurate features at  $L = (0, 0, 0.9)$  and  $L = (0, 0, 1.15)$  are powder rings most likely from CrNiAl alloy.

a good neutron transmission for thermal neutrons. Similarly, we have measured the ratio of the integrated intensities for  $k_f = 1.141 \text{ \AA}^{-1}$  and found the transmission for cold neutrons to be  $\sim 0.09$ , making it possible to collect sufficient inelastic scattering statistics in a reasonable time. The measured transmission figures agree well with those calculated from the composition of the alloys used and cell dimensions.

The onset of ferromagnetism in UGe<sub>2</sub> is marked by an increase of the intensity of elastic scattering at the  $(0, 0, 1)$  position in reciprocal space. We have collected longitudinal elastic scans through  $Q = 2\pi(0, 0, L)/c$  at temperatures between 3 K and 60 K ( $c = 4.116 \text{ \AA}$  at  $T = 297$  K) in order to measure the temperature dependence of the magnetic scattering (Fig. 7). The measurements at  $Q = 2\pi(0, 0, 1)/c$  show the expected increase in intensity at low temperature due to magnetic ordering (the small residual intensity at 45 K is due to a finite nuclear scattering contribution at  $(0, 0, 1)$ ). At this pressure the ordering temperature is suppressed from 52.6 K at ambient pressure to 37 K. Two broad features at  $Q = 2\pi(0, 0, 0.9)/c$  and  $Q = 2\pi(0, 0, 1.15)/c$  are temperature independent. Rocking curves collected at  $Q = 2\pi(0, 0, 0.9)/c$  and  $Q = 2\pi(0, 0, 1.15)/c$  revealed that these features did not vary with the rotation of the sample and we attribute them to powder rings from the CrNiAl alloy used in the cell.

An example of inelastic neutron scattering data collected at high pressure is presented in Fig. 8, which illustrates the statistics that can be obtained during  $\sim 45$  min data collection. The energy scans at  $Q = 2\pi/c(0, 0, 1 - \delta)$  are plotted at temperatures below, at, and above  $T_C$ . At 1.1 GPa the  $T_C$  of UGe<sub>2</sub> is reduced to 37 K, and accordingly the magnetic

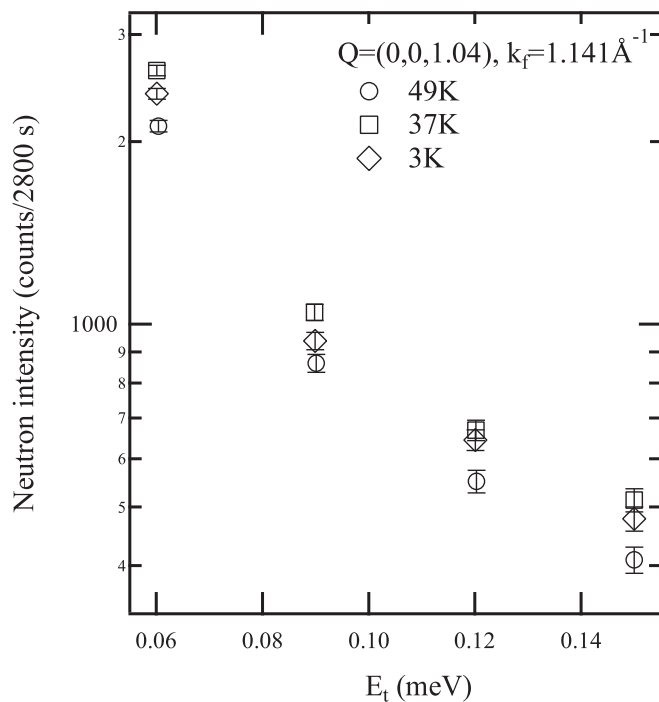


FIG. 8. Magnetic critical scattering in  $\text{UGe}_2$  under pressure. Energy scans performed at 1.1 GPa at  $Q = 2\pi/c(0, 0, 1 - \delta)$  at temperatures above and below  $T_C$  as well as at  $T_C = 37$  K.

critical scattering is expected to be a maximum at 37 K, a result we find to be true at all energy transfers probed in our measurements. The full results of this experiment will be published elsewhere.

## VI. CONCLUSIONS

We have built and tested a clamped high-pressure cell suitable for collecting data in inelastic neutron scattering experiments. The cell combines a large sample volume of  $\sim 425$  mm<sup>3</sup> with a safe operating pressure limit of 1.8 GPa. The design of the cell has been optimised using finite element analysis. The novel seal design eliminates the need for a sample container. The plug with the manganin pressure gauge used in the pressure cell provides an accurate reading of pressure at any given temperature and pressure and eliminates the need for a pressure reference material in the neutron beam. The performance of the cell was demonstrated for inelastic neutron scattering studies on  $\text{UGe}_2$  for which it can be used to access the entire magnetic and superconducting  $P$ - $T$ -phase diagram.

## ACKNOWLEDGMENTS

The authors would like to thank Mr. Andrew Downie (School of Physics and Astronomy, University of Edinburgh) for his technical assistance. The work is funded by the Engineering and Physical Sciences Research Council (Grant No. EP/E063985/1) and the Science and Technology Facilities Council (UK) (Grant No. ST/F001495/1). A.D.H. acknowledges support from the Royal Society.

- <sup>1</sup>G. L. Squires, *Introduction to the Theory of Thermal Neutron Scattering* (Dover, New York, 1997).
- <sup>2</sup>S. S. Saxena, P. Agarwal, K. Ahilan, F. M. Grosche, R. K. W. Haselwimmer, M. J. Steiner, E. Pugh, I. R. Walker, S. R. Julian, P. Monthoux, G. G. Lonzarich, A. Huxley, I. Sheikin, D. Braithwaite, and J. Flouquet, *Nature (London)* **406**, 587 (2000).
- <sup>3</sup>A. Huxley, I. Sheikin, E. Ressouche, N. Kernavanois, D. Braithwaite, R. Calemczuk, and J. Flouquet, *Phys. Rev. B* **63**, 144519 (2001).
- <sup>4</sup>A. D. Huxley, S. Raymond, and E. Ressouche, *Phys. Rev. Lett.* **91**, 207201 (2003).
- <sup>5</sup>S. Raymond, and A. D. Huxley, *Physica B* **350**, 33 (2004).
- <sup>6</sup>T. Hong, V. O. Garlea, A. Zheludev, and J.A. Fernandez-Baca, *Phys. Rev. B* **78**, 224409 (2008).
- <sup>7</sup>C. Pfleiderer, A. D. Huxley, and S.M. Hayden, *J. Phys.: Condens. Matter* **17**, S3111 (2005).
- <sup>8</sup>J. Paureau and C. Vettier, *Rev. Sci. Instrum.* **46**, 11 (1975).
- <sup>9</sup>R. Done, M. Chowdhury, C. Goodway, M. Adams, and O. Kirichek, *Rev. Sci. Instrum.* **79**, 26107 (2008).
- <sup>10</sup>J.-P. Pinceaux, J.-P. Maury, and J.-M. Besson, *J. Phys. Lett.-Paris* **40**, L307 (1979).
- <sup>11</sup>S. Klotz, J. M. Besson, G. Hamel, R. J. Nelmes, J. S. Loveday, and W.G. Marshall, *High Press. Res.* **14**, 249 (1996).
- <sup>12</sup>S. Klotz, M. Braden, and J.M. Besson, *Hyperfine Interact.* **128**, 245 (2000).
- <sup>13</sup>See <http://www.ill.eu/> for ILL Clamped Cell 04PCL150CB5.
- <sup>14</sup>A. Sieber, G. Chaboussant, R. Bircher, C. Boskovic, and H. Güdel, *Phys. Rev. B* **70**, 172413 (2004).
- <sup>15</sup>A. Sieber, R. Bircher, O. Waldmann, G. Carver, G. Chaboussant, H. Mutka, and H. Güdel, *Angew. Chem. Int. Ed.* **44**, 4339 (2005).
- <sup>16</sup>See <http://www.ngkberylco.co.uk/> for NGK Berylco U.K. Ltd.
- <sup>17</sup>B. Få, K. R. A. Sadykov, J. Flouquet, and G. Lapertot, *J. Phys.: Condens. Matter* **17**, 1635 (2005).
- <sup>18</sup>D. L. Decker, *J. Appl. Phys.* **36**, 1 (1965).
- <sup>19</sup>A. Eiling and J. S. Schilling, *J. Phys. F: Met. Phys.* **11**, 623 (1981).
- <sup>20</sup>See <http://www.kennametal.com/> for Kennametal Inc.
- <sup>21</sup>B. V. Motovilov, *Precision Alloys* (Metallurgiya, Moscow, 1983).
- <sup>22</sup>M. Eremets, *High Pressure Experimental Methods* (Oxford University Press, Oxford, 1996).
- <sup>23</sup>See <http://www.ansys.com/> for ANSYS®, Inc.
- <sup>24</sup>See <http://www.solidedge.com/> for SOLID EDGE.
- <sup>25</sup>I.R. Walker, *Rev. Sci. Instrum.* **70**, 8 (1999).
- <sup>26</sup>N. Fujiwara, T. Matsumoto, K. Koyama-Nakazawa, Y. Uwatoko, A. Hisada, Y. Fujimaki, and S. Uchida, *J. Phys.: Conf. Ser.* **121**, 122004 (2008).
- <sup>27</sup>S. E. McLain, M. R. Dolgos, D. A. Tennant, J. F. C. Turner, T. Barnes, Th. Proffen, B. C. Sales, and R. I. Bewley, *Nature Materials* **5**, 561 (2006).
- <sup>28</sup>L.H. Dmowski, and E. Litwin-Staszewska, *Meas. Sci. Technol.* **10**, 343 (1999).
- <sup>29</sup>H. Taniguchi, S. Takeda, R. Satoh, A. Taniguchi, H. Kamatsu, and K. Satoh, *Rev. Sci. Instrum.* **81**, 033903 (2010).